Available online at www.sciencedirect.com
ScienceDirect
Polymer 48 (2007) 7249–7254
polymer
www.elsevier.com/locate/polymer

Drastic ligand electronic effect on anilido–imino nickel catalysts toward ethylene polymerization

Haiyang Gao [a], Zuofeng Ke [a], Lixia Pei [b], Keming Song [a], Qing Wu [a],*

[a] Institute of Polymer Science, School of Chemistry and Chemical Engineering, Sun Yat-sen (Zhongshan) University, Guangzhou 510275, China
[b] School of Chemical and Energy Engineering, South China University of Technology, Guangzhou 510641, China

Received 27 July 2007; received in revised form 25 September 2007; accepted 17 October 2007
Available online 23 October 2007

Abstract

A novel nitro–anilido–imino nickel complex ($(Ar^1N{=}CHC_6H_3(\text{-}5\text{-}NO_2)NAr^2)NiBr$) ($Ar^1 = Ar^2 =$ 2,6-dimethylphenyl) was designed, synthesized, and characterized to investigate ligand electronic effect on late transition metal olefin polymerization catalysts. As a catalyst for ethylene polymerization, neutral anilido–imino nickel complex with an electron-withdrawing nitro group showed good activity (442.1 kg $(\text{mol Ni h})^{-1}$) with MAO as cocatalyst. The catalytic activity and molecular weight of the obtained products were significantly affected by electronic effect of the anilido–imine ligand. Theoretical calculations suggested that ligand electronic effect led to different charge distribution on the nickel metal atom, and the catalytic activity predominantly increased with an increase in electrophilicity of the nickel metal center.

Keywords: Anilido–imino nickel complexes; Calculations; Electronic effect

1. Introduction

In late transition metal olefins polymerization catalyst design, ligand steric effect plays an important role in determining the catalytic activity and polymer molecular weight [1–5]. To suppress the facial chain transfer, many bulky late transition metal complexes have been developed as highly active olefin polymerization catalysts [6–11]. However, steric effect is not an exclusive crucial factor to determine the catalytic activity, influence of ligand electronic effect on catalytic activity has been observed in many catalytic systems [12–26]. By studying the influence of the steric and electronic effects of ligands on catalytic activity in a $(CpR)_2ZrCl_2$/ethylaluminoxane catalysis system, Möhring and Coville concluded that the electronic effect could contribute as much as 80% to the change in polymerization activities [12]. It was shown that the catalytic activity of metallocene catalyst increased with reduced net charge [13,14]; while the catalytic activity of α-diimine Ni(II) catalyst increased along with the net charge [6,15–17]. Experimental results and theoretical calculations also indicated that substituents on backbone of the salicylaldiminate ligand had a significant influence on the activity for ethylene polymerization [18–22]. Fujita believed that highly active olefin polymerization catalysts could be achieved by moderate electron-donating properties of ligands, and *FI* catalysts were discovered as a result of ligand-oriented catalyst design [23]. Fujita and Coates have also reported the effect of electron-withdrawing groups for bis(phenoxyimine) titanium catalyst: fluorine substitution at the *ortho* positions of the ligand *N*-aryl ring results in living behavior, while substitution at the *meta* or *para* positions increases catalyst activity [24–26].

From a view point of steric effect, we previously synthesized a series of bulky anilido–imino nickel complexes ($(Ar^1N{=}CHC_6H_4NAr^2)NiBr$) ($Ar^1 = Ar^2 =$ 2,6-dimethylphenyl, **1**; $Ar^1 =$ 2,6-dimethylphenyl, $Ar^2 =$ 2,6-diisopropylphenyl, **2**; $Ar^1 = Ar^2 =$ 2,6-diisopropylphenyl, **3**; $Ar^1 =$ 2,6-diisopropylphenyl, $Ar^2 =$ 2,6-dimethylphenyl, **4**) (Scheme 1), and investigated their catalytic behaviors toward olefin polymerization

---

* Corresponding author. Tel.: +86 020 84113250; fax: +86 020 84114033.
E-mail address: ceswuq@mail.sysu.edu.cn (Q. Wu).

0032-3861/$ - see front matter © 2007 Elsevier Ltd. All rights reserved.
doi:10.1016/j.polymer.2007.10.022

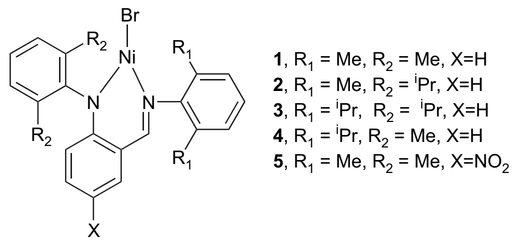

Scheme 1. Structure of anilido–imino nickel complexes.

[27–30]. Bulky anilido–imino nickel complexes showed low activities for ethylene oligomerization [27], while salicylaldiminato [18,19] and β-diketiminato [31] nickel complexes showed moderate activities for ethylene polymerization, which is beyond our anticipation. In comparison of salicylaldiminate ligands with anilido–imine ligands, the latter have greater steric effect, but the negative charge of the phenoxy group (PhO^-) is larger than that of the anilido group (PhN^-–) according to the calculations by PM3/MNDO method [23]. Similarly, in comparison of β-diketiminate ligands with anilido–imine ligands, both nearly have the same steric hindrance, but the latter have a conjugated benzene ring which is a strong electron-donating group. Therefore, we speculated that low electrophilic nature of the anilido–imino nickel metal center should be responsible for low ethylene oligomerization activity.

From a view point of electronic effect, we herein designed and synthesized a novel nitro–anilido–imino nickel complex **5** ($Ar^1N{=}CHC_6H_3(\text{-}5\text{-}NO_2)NAr^2$)NiBr ($Ar^1 = Ar^2 =$ 2,6-dimethylphenyl) (Scheme 1) by introducing an electron-withdrawing nitro group, and investigated its catalytic behaviors toward ethylene polymerization. Experimental data and theoretical calculations showed consistently that ligand electronic effect had drastic influence on the catalytic activity and molecular weight of the obtained polymer.

2. Experimental part

2.1. General methods and materials

All manipulations involving air- and moisture-sensitive compounds were carried out under an atmosphere of dried and purified nitrogen using standard vacuum-line, Schlenk or drybox techniques. Toluene, hexane and THF were dried over sodium metal and distilled under nitrogen; benzene-d_6 was dried over CaH_2. 2-Fluorobenzaldehyde (97%), 1,2-dimethoxyethane (99%), anhydrous nickel(II) bromide (99%) and 2,6-dimethylaniline were bought from Aldrich Chem. Co. and used without further purification. Methylaluminoxane (MAO) was prepared by partial hydrolysis trimethylaluminum (TMA) in toluene at 0–60 °C with $Al_2(SO_4)_3 \cdot 18H_2O$ as water source. The initial $[H_2O]/[TMA]$ molar ratio was 1.3. (DME)$NiBr_2$ was synthesized by the direct reaction of 1,2-dimethoxyethane with anhydrous nickel(II) bromide. The anilido–imine ligands and corresponding nickel complexes **1–4** were prepared according to our previous methods [27]. Salicylaldiminato–Ni(II) (3 position substituent R = 9-phenanthrenyl), and β-diketiminato–Ni(II) complexes were prepared following literature procedure [18,31]. Other commercially available reagents were purchased and used without purification.

2.2. Ethylene polymerization

A mechanically stirred 100 mL Parr reactor was heated overnight to 150 °C under vacuum and then cooled to room temperature. The autoclave was pressurized to 10 atm of ethylene and vented three times. The autoclave was then charged with 25 mL of a toluene solution of MAO under 1 atm of ethylene at initialization temperature. The system was maintained by continuously stirring for 30 min, and then the nickel complex solution was charged into the autoclave under 1 atm of ethylene. The ethylene pressure was raised to the specified value, and the reaction was carried out for a certain time. Polymerization was terminated by addition of acidic ethanol after releasing ethylene pressure. The resulting precipitated polymers were collected and treated by filtering, washing with ethanol several times, and drying under vacuum at 60 °C to a constant weight. The organic fraction was separated and filtered through a plug of activated alumina, and a small sample of the organic layer was dried over anhydrous Na_2SO_4 and then analyzed by GC–MS.

2.3. Characterization

Elemental analyses were performed on a Vario EL microanalyzer. Mass spectra were measured on a LCQ DECA XP LC/MS instrument using electro spray ionization (EI). NMR spectra were carried out on an INOVA 500 MHz at room temperature in $CDCl_3$ solution for organic compounds and in C_6D_6 solution for complex. ^{13}C NMR spectra of the polyethylene samples were carried out on an INOVA 500 MHz instrument operating at 125 MHz at 120 °C in *o*-dichlorobenzene and *o*-dichlorobenzene-d_4 (20% v/v) in 10 mm sample tube. High-temperature gel permeation chromatography (GPC) analyses of the molecular weight and molecular weight distribution (MWD) of the polymers were performed on a Waters Alliance GPC2000 instrument using standard polystyrene as the reference and with trichlorobenzene (TCB) as the eluent at 135 °C. DSC analyses were conducted with a PerkinElmer DCS-7 system. The DSC curves were recorded from −50 °C to 150 °C at a heating rate of 10 °C/min and a cooling rate of 10 °C/min. Analyses of ethylene oligomers were performed by GC–MS on a Finnigan Voyager GC-8000 TOP gas chromatograph–mass spectrometer.

2.4. Crystal structure determination

Crystal data obtained with the $\omega - 2\theta$ scan mode were collected on a Bruker SMART 1000 CCD diffractometer with graphite-monochromated Mo Kα radiation ($\lambda = 0.71073$ Å) at 293 K. The structure was solved using direct methods, while further refinements with full-matrix least squares on F^2 were obtained with the SHELXTL program package. All non-hydrogen atoms were refined anisotropically. Hydrogen atoms were introduced in calculated positions with the displacement factors of the host carbon atoms.

2.5. Computational method

The ONIOM (our own *n*-layered integrated molecular orbital and molecular mechanics) method [32] was employed to investigate the electronic structures of complexes involved in the insertion process for the salicylaldiminato–Ni(II), β-diketiminato–Ni(II), anilido–imino–Ni(II) and nitro–anilido–imino–Ni(II) complexes. According to a commonly accepted Cossee mechanism of the catalytic polymerization [33,34], the polymerization initiates by an active species with a vacant site, which is generated from the activation of the precursors in the presence of MAO. The olefin coordination to the central metal or insertion into the M–P bond (M: metal center, P: growing chain) is a turnover step, thus methyl is chosen as a model substitute to represent the growing chain on the active center during polymerization. In the calculations, all the atoms which were sensitive to the electronic nature of the metal center, including the M–CH_3 and the ligands without the bulky substituents on N atoms, were treated at the B3LYP/6-31G* level of theory [35,36]. The substituents on N atoms were treated by the UFF without the electrostatic contribution [37]. All the optimizations were carried out using the Gaussian 03 program without any symmetry constraints [38]. Analytical frequency calculations at the same level were done in order to confirm the optimized structures to be a minimum.

2.6. Syntheses of ligand **L5** and complex **5**

2.6.1. Synthesis of 2-F–5-NO_2–C_6H_3CHO

KNO_3 (22.22 g, 0.22 mol) was dissolved in 200 mL sulfuric acid (98%) at ice bath, then 21.2 mL (0.22 mol) 2-fluorobenzaldehyde was dropped into the mixtures and stirred for 5 h. The obtained products were dumped into cracked ice, the pale yellow precipitation was collected by filtrating and washing with water until pH = 7. The precipitation was recrystallized in hot ethanol to give 30.4 g colorless crystals. Yield: 90%. MS (*m*/*z*): 170.2 $[M]^+$. ^1H NMR (500 MHz, $CDCl_3$): δ (ppm) = 10.36 (1H, CHO), 8.75 (1H, 6-H), 8.49 (1H, 4-H), 7.39 (1H, 3-H). ^{13}C NMR (125 MHz, $CDCl_3$): δ (ppm) = 184.83, 169.08, 165.53, 144.91, 131.18, 125.06, 118.54. Anal. Calcd. for $C_7H_4FNO_3$: C, 49.56; H, 2.21; N, 8.07. Found: C, 49.72; H, 2.38; N, 8.28.

2.6.2. Synthesis of 2-F–5-NO_2–C_6H_3(CH=NC_6H_4–2,6-Me_2)

A 13.74 g (81.30 mmol) portion of 2-fluoro-5-nitro-benzaldehyde and 11 mL (89.43 mmol) 2,6-dimethylaniline in 30 mL ethanol were stirred for 2 h, the resulting yellow precipitations were collected by filtration and then recrystallized in ethanol to give 14.80 g small yellow crystals. Yield: 67%. MS (*m*/*z*): 273.2 $[M]^+$. ^1H NMR (500 MHz, $CDCl_3$): δ (ppm) = 9.10 (1H, CH=NAr), 8.50 (1H, Ph), 8.33 (1H, Ph), 7.29 (1H, Ph), 7.07–7.04 (2H, Ph), 6.98–6.93 (1H, Ph), 2.13 (6H, Me). ^{13}C NMR (125 MHz, $CDCl_3$): δ (ppm) = 167.34, 163.86, 154.13, 150.48, 145.01, 128.45, 128.10, 127.96, 127.02, 124.08, 124.02, 117.70, 117.38, 18.67. Anal. Calcd. for $C_{16}H_{16}FN_2O_2$: C, 66.05; H, 4.63; N, 10.11. Found: C, 66.17; H, 4.81; N, 10.29.

2.6.3. Synthesis of ligand **L5** (Ar^1N=CHC_6H_3(-5-NO_2)NHAr^2) ($Ar^1 = Ar^2$ = 2,6-dimethylphenyl)

n-Hexane solution (21 mL) of *n*-butyllithium (2.6 M) was dropped into a solution of 2,6-dimethylaniline (7.7 mL) in THF (50 mL) at −78 °C, and allowed to warm to room temperature overnight. The resulting solution of LiNHAr was cannula-transferred into a solution of 2-F–5-NO_2–C_6H_3(CH=NC_6H_4–2,6-Me_2) (14.8 g) in 30 mL THF at 25 °C. After stirring for 2 h, the reaction was quenched with 20 mL H_2O, and evaporated to dryness. The resulting solid was extracted with hot ethanol, and the obtained ethanol solution was evaporated to dryness to give the yellow solid. This product was recrystallized in ethanol–THF solvent (9:1, v/v) to give 5.1 g yellow crystals. Yield: 25.3%. MS (*m*/*z*): 374.4 $[M]^+$. ^1H NMR (500 MHz, $CDCl_3$): δ (ppm) = 11.42 (1H, NH), 8.43 (1H, CH=NAr), 8.33 (1H, Ph), 8.05 (1H, Ph), 7.17 (3H, Ph), 7.10–7.08 (2H, Ph), 6.99 (2H, Ph), 6.29 (1H, Ph), 2.21 (12H, Me). ^{13}C NMR (125 MHz, $CDCl_3$): δ (ppm) = 160.13, 148.42, 144.90, 132.51, 131.54, 130.93, 126.88, 124.21, 123.79, 123.38, 123.14, 122.84, 120.06, 110.82, 107.08, 14.12. Anal. Calcd. for $C_{24}H_{26}N_3O_2$: C, 73.75; H, 6.12; N, 11.04. Found: C, 73.97; H, 6.21; N, 11.25.

2.6.4. Synthesis of complex 5 (Ar^1N=CHC_6H_3(-5-NO_2)NAr^2)NiBr ($Ar^1 = Ar^2$ = 2,6-dimethylphenyl)

A 1.64 g portion of **L5** was dissolved in 50 mL toluene in a flame-dried Schlenk flask, and 2 mL *n*-butyllithium (2.6 M) was injected in a −78 °C dry ice/acetone bath, which was warmed to room temperature overnight. (DME)$NiBr_2$ (1.34 g) was added, and then stirred for 24 h at room temperature, the crude reaction mixtures were followed by filtration under nitrogen. The resulting dark brown solution was evaporated to low volume in vacuo, and then *n*-hexane (15:1) was added. Solvent was removed from the precipitate *via* cannula filtration, and the residual brown solid was washed with *n*-hexane (3 × 5 mL). Drying in vacuo produced the desired nickel complex **5**. Yield: 32%. MS (*m*/*z*): 510, 511, 512, 513, 514, 515 (isotope, $[M]^+$); 429, 430, 431, 432, 433 (isotope, $[M - Br]^+$); 374 (ligand$^+$). ^1H NMR (C_6D_6, 500 MHz): δ (ppm) = 48.01 (2H, Ph), 47.12 (6H, CH_3), 45.36 (2H, Ph), 44.00 (6H, CH_3), 36.48 (2H, Ph), 21.26 (1H, CH=N), −12.18 (1H, backbone benzene), −26.66 (1H, backbone benzene), −44.77 (1H, backbone benzene). Anal. Calcd. for $C_{23}H_{22}N_3O_2NiBr$: C, 53.68; H, 4.67; N, 7.95. Found: C, 54.16; H, 4.34; N, 8.22.

3. Results and discussion

The yellow nirtro–anilido–imine ligand **L5** was synthesized by nitration, condensation (Schiff base reaction), and nucleophilic aromatic displacement reactions (Scheme 2). Anchored by fluoro and aldehyde groups, nitro group was introduced at 5 position of benzene ring in high yield (~90%). The structure of ligand was confirmed by MS, NMR, and

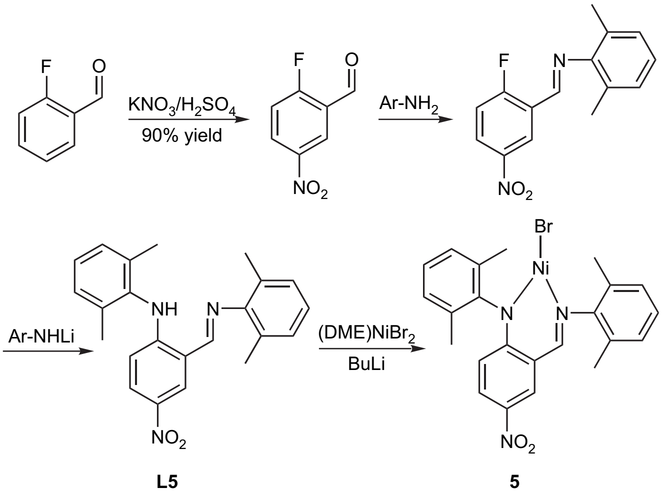

Scheme 2. Preparation of nickel complex **5**.

elemental analysis. A single crystal of **L5** (Fig. 1) also confirmed that nitro group was introduced assuredly at 5 position [39]. Attempt to synthesize more bulky ligand ($Ar^1N{=}CHC_6H_3(\text{-}5\text{-}NO_2)NHAr^2$; $Ar^1 = Ar^2 =$ 2,6-diisopoylphenyl) following similar synthetic route was unsuccessful because bulky hindrance and passivation of nitro group retarded nucleophilic aromatic displacement reaction.

After the ligand **L5** was treated with *n*-butyllithium in toluene, 1.1 equiv. of (DME)NiBr$_2$ was added to the solutions and nitro–anilido–imino nickel complex **5** was obtained as brown solids. The structure of **5** was confirmed by elemental analysis, MS, and ^{1}H NMR spectrum. Similar to complexes **1–4**, **5** also exhibits a broadened ^{1}H NMR spectrum from 48 to −45 ppm, but the spectrum width of **5** is narrower than that of **1–4** due to the electron-withdrawing effect of nitro group [40,41].

Our previous experiment results indicated that bulky anilido–imino complexes **1–4** showed low activities for ethylene oligomerization with MAO as cocatalyst [27]. Experimental data in Table 1 further suggested that catalytic activity increased, and the higher olefins were produced with increase in ethylene pressure and ligand steric hindrance. Oligomers catalyzed by **1**/MAO at 10 atm ethylene pressure consist of 55% (C4), 29% (C6), 10% (C8), and 6% (≥C10). However, **5** with an electron-withdrawing nitro group showed good activities for ethylene polymerization with MAO as cocatalyst. It could be seen that **5** showed a significant increase in catalytic activity comparing to its counterpart **1** at 1 atm pressure, which is consistent with our anticipation. At 10 atm polymerization pressure, **5** showed *ca.* 20 times higher catalytic activity than that of **1**, and the obtained products were the polyethylene with high molecular weight.

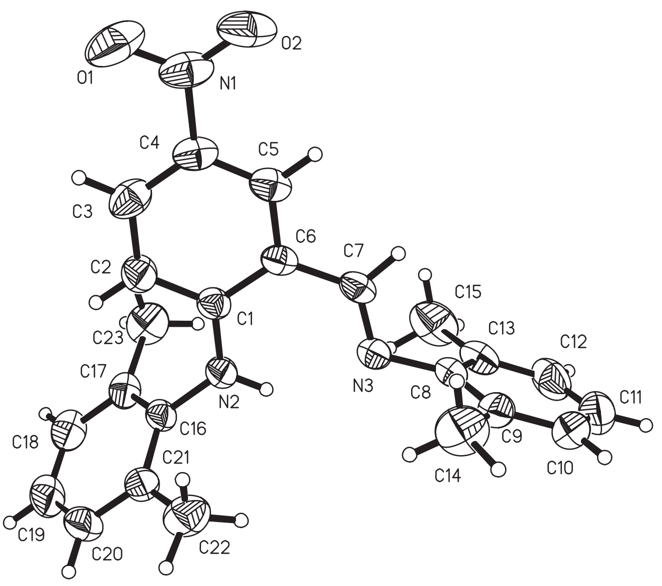

Fig. 1. ORTEP plot of ligand **L5**.

Table 1
Ethylene oligomerization or polymerization catalyzed by **1**, **3**, and **5**/MAO

Catalysts	Ethylene pressure (atm)	Activity (kg (mol Ni h)$^{-1}$)	Oligomers (mol%)[a]			
			C4	C6	C8	≥C10
1	1	1.3	61	34	5	
1	10	3.8	55	29	10	6
3	1	2.1	58	33	9	
3	10	4.9	48	30	13	9
5	1	5.2	PE with $M_w = 13.2 \times 10^4$			
5	10	73.5	PE with $M_w = 18.4 \times 10^4$			

Reaction conditions: catalyst addition: 20 μmol for **1** and **3**, 10 μmol for **5**; Al/Ni = 150; reaction time: $t = 1$ h; polymerization temperatures $T_p = 30$ °C; solution: 30 mL toluene.

[a] Oligomers compositions were determined by GC–MS, and molecular weights of the PEs were determined by GPC in trichlorobenzene at 135 °C.

Obviously, the differences in their activity and molecular weight of product are due to special electronic effect of the 5-nitro substituents. To further confirm our previous speculation, ONIOM method [32,42] was employed to investigate the electronic structures of the complexes involved in the insertion process for salicylaldiminato–Ni(II), β-diketiminato–Ni(II), and anilido–imino–Ni(II) complexes.

Optimized results showed all of complexes involved in the insertion process had an approximate planar square coordinated structure with a vacant site. Mulliken atomic charges (MAC) analyses showed that ligand structures led to different charge distribution on the nickel metal center. There is a very interesting correlation between the charges on the nickel metal center and their catalytic activities for ethylene polymerization (Table 2). Salicylaldiminato–Ni(II) had the most positive metal center (MAC = 0.633), thus it showed the highest catalytic activity for ethylene polymerization (121 kg (mol Ni h)$^{-1}$).

Table 2
Mulliken atomic charge analyses of electronic structures of the complexes involved in the insertion process (B3LYP/6-31G* Level of Theory)

Complexes[a]	MACs on Ni	Activity (kg (mol Ni h)$^{-1}$)
Salicylaldiminato–Ni(II)	0.633	121
β-Diketiminato–Ni(II)	0.592	79.4
Anilido–imino–Ni(II)	0.586	6.1
Nitro–anilido–imino–Ni(II)	0.600	106

Polymerization condition: catalyst addition: 10 μmol; ethylene pressure: 10 atm; Al/Ni = 400; $T_p = 30$ °C; solvent: 30 mL toluene; reaction time: 1 h.

[a] Aryl substituent of complexes: Ar = 2,6-dimethylphenyl, 3 position substituent of salicylaldiminato–Ni(II) is 9-phenanthrenyl.

β-Diketiminato–Ni(II) had the relative negative metal center (MAC = 0.592), experimental study showed that it exhibited a moderate catalytic activity (79.4 kg (mol Ni h)$^{-1}$). Anilido–imino–Ni(II) had the most negative metal center (MAC = 0.586), it exhibited a low catalytic activity (6.1 kg (mol Ni h)$^{-1}$) for ethylene oligomerization. The introduction of nitro group on anilido–imine ligand resulted in an increase of the MAC on the nickel center from 0.586 to 0.600, thus catalytic activity for ethylene polymerization increased by a factor of 17.

For anilido–imino nickel catalytic systems, a reasonable explanation for the catalytic activity enhancement and molecular weight of product increase is that the presence of electron-withdrawing groups would reduce the electron density on the metal sites and generate a more electrophilic nickel center, thus reducing activation energy for ethylene insertion, and favoring the olefin coordination and insertion in the growing chain and hence limiting the tendency to chain termination *via* β-hydrogen elimination [22].

For **5**/MAO catalytic system, the reaction temperature and Al/Ni ratio affected the catalytic activities for ethylene polymerization. The polymerization results were reproduced several times and were collected in Table 3. With an increase in the reaction temperature, the catalytic activity for ethylene polymerization increased, and then decreased. When temperature was up to 30 °C, the catalytic activity decreased obviously, and a small quantity of elastomeric polymer was obtained. This suggests that the decrease in activity can be ascribed to a decrease in ethylene solubility at increased temperatures, and the high temperature favors formation of highly branched polyethylene [6,31]. With an increase in Al/Ni ratio, the catalytic activities for ethylene polymerization increased, and then decreased. On the optimum polymerization condition ($T = 10$ °C and Al/Ni = 400), catalytic activity was up to 31.8 kg (mol Ni h)$^{-1}$ at 1 atm polymerization pressure, and weight-average molecular weight of the obtained polyethylene reached 28.4×10^4. At 10 atm polymerization pressure, the higher catalytic activity (442.1 kg (mol Ni h)$^{-1}$) was obtained.

Table 3
Results of ethylene polymerization catalyzed by **5**/MAO

Run	T_p (°C)	Al/Ni ratio (mol/mol)	Activity (kg (mol Ni h)$^{-1}$)	M_w[a] (10^4)	MWD[a]	Branches/ 1000C[b]	T_m[c] (°C)
1	−5	150	0.7	42.3	2.99	12	129
2	10	150	16.3	31.7	3.38	39	98
3	20	150	13.1	19.5	3.08	43	87
4	30	150	5.2	13.2	3.29	61	54
5	50	150	2.6				–
6	10	100	7.1				
7	10	300	25.2				
8	10	400	31.8	28.4	3.27	41	93
9	10	500	20.9				
10[d]	10	400	442.1	33.6	3.12	28	115

Polymerization condition: catalyst addition: 10 μmol; ethylene pressure: 1 atm; solvent: 30 mL toluene; reaction time: $t = 1$ h.

[a] M_w and MWD of the PEs were determined by GPC in trichlorobenzene at 135 °C.

[b] Determined by ^{13}C NMR spectra of polyethylene.

[c] Determined by DSC.

[d] Catalyst addition: 5 μmol; ethylene pressure: 10 atm.

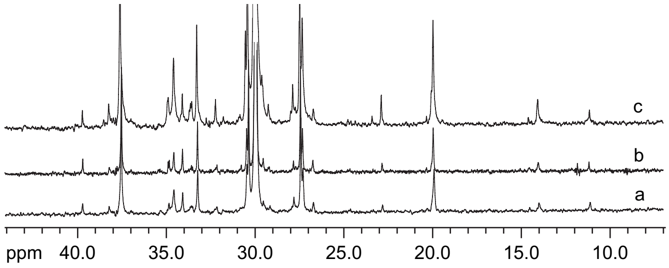

Fig. 2. ^{13}C NMR spectra of polyethylenes catalyzed by **5**/MAO at various temperatures: (a) 10 °C; (b) 20 °C; and (c) 30 °C.

In addition, ^{13}C NMR spectra showed that the products catalyzed by **5**/MAO are methyl-rich-branched polyethylene (Fig. 2), and the corresponding branches' resonance peaks including methyl, ethyl, propyl, butyl, pentyl, and long branched chains ($n \geq 6$) can be found. The branching numbers of the polyethylenes increase with temperature, while their molecular weight and melting point (T_m) decrease correspondingly. This is in good agreement with reported results by Brookhart groups, and the formation of the branches can be illustrated by chain walking mechanism [2–4,6].

4. Conclusions

In summary, we have successfully designed and synthesized a good ethylene polymerization catalyst **5** from a view point of electronic effect. It is noteworthy that electronic effect of the anilido–imine ligand plays a dominant role in determining the catalytic activity and molecular weight of the polymers. Theoretical calculations by ONIOM method also further confirmed that ligand electronic effect led to different charge distribution on the nickel metal atom, and catalytic activities predominantly increased with an increase of electrophilicity in the nickel metal center. On the optimum polymerization condition ($T = 10$ °C and Al/Ni = 400), the catalytic activity of **5**/MAO system is up to 442.1 kg (mol Ni h)$^{-1}$. The obtained products are methyl-rich-branched polyethylene.

Acknowledgements

We thank financial support from the National Natural Science Foundation of China (NSFC) and SINOPEC (Joint-Project 20334030), NSFC (Projects 20604034), and the Science Foundation of Guangdong Province (Projects 039184, 06300069).

References

[1] Ittel SD, Johnson LK, Brookhart M. Chem Rev 2000;100:1169.
[2] Johnson LK, Killian CM, Brookhart M. J Am Chem Soc 1995;117:6414.
[3] Johnson LK, Mecking S, Brookhart M. J Am Chem Soc 1996;118:267.
[4] Mecking S, Johnson LK, Wang L, Brookhart M. J Am Chem Soc 1998;120:888.
[5] Gibson VC, Sptizmesser SK. Chem Rev 2003;103:238.
[6] Gates DP, Svejda SA, Onate E, Killian CM, Johnson LK, White PS, et al. Macromolecules 2000;33:2320.

[7] Ionkin AS, Marshall WJ. Organometallics 2004;23:3276.
[8] Ionkin AS, Marshall WJ. J Organomet Chem 2004;689:1057.
[9] Zuidevild MA, Wehrmann P, Röhr C, Mecking S. Angew Chem Int Ed 2004;43:869.
[10] Britovsek GJP, Gibson VC, Kimberley BS, Maddox PJ, Mctavish SJ, Solan GA, et al. Chem Commun 1998:849.
[11] Camacho DH, Salo EV, Guan Z, Ziller JW. Organometallics 2005;24:4933.
[12] Möhring PC, Coville NJ. J Mol Catal 1992;77:41.
[13] Guo D, Yang X, Yang L, Liu T, Li Y, Hong H, et al. J Polym Sci Part A Polym Chem 2000;38:2232.
[14] Guo D, Yang X, Liu T, Hu Y. Macromol Theory Simul 2001;10:75.
[15] Guo D, Han L, Zhang T, Sun W, Li T, Yang X. Macromol Theory Simul 2002;11:1006.
[16] Popeney C, Guan Z. Organometallics 2005;24:1145.
[17] Zhang L, Brookhart M, White PS. Organometallics 2006;25:1868.
[18] Younkin TR, Connor EF, Henderson JI, Friedrich SK, Grubbs RH, Bansleben DA. Sciences 2000;287:460.
[19] Wang C, Friedrish S, Younkin TR, Grubbs RH. Organometallics 1998;17:3149.
[20] Chan MSW, Deng L, Ziegler T. Organometallics 2000;19:2741.
[21] Zhang T, Guo D, Jie S, Sun W, Li T, Yang X. J Polym Sci Part A Polym Chem 2004;42:4765.
[22] Carlini C, Macinai A, Masi F, Galletti AMR, Santi R, Sbrana G, et al. J Polym Sci Part A Polym Chem 2004;42:2534.
[23] Makio H, Kashiwa N, Fujita T. Adv Synth Catal 2002;5:344.
[24] Mitani M, Mohri J, Yoshida Y, Saito J, Ishii S, Ysuru K, et al. J Am Chem Soc 2002;124:3327.
[25] Mason AF, Tian J, Hustad PD, Lobkovsky EB, Coates GW. Isr J Chem 2002;42:301.
[26] Mason AF, Coates GW. J Am Chem Soc 2004;126:10798.
[27] Gao H, Guo W, Bao F, Gui G, Zhang J, Zhu F, et al. Organometallics 2004;23:6273.
[28] Gao H, Zhang J, Chen Y, Zhu F, Wu Q. J Mol Catal A Chem 2005;240:178.
[29] Gao H, Chen Y, Zhu F, Wu Q. J Polym Sci Part A Polym Chem 2006;44:5237.
[30] Gao H, Pei L, Song K, Wu Q. Eur Polym J 2007;43:908.
[31] Zhang J, Ke Z, Bao F, Long J, Gao H, Zhu F, et al. J Mol Catal A Chem 2006;249:31.
[32] Svensson M, Humbel S, Froese RDJ, Matsubara T, Sieber S, Morokuma K. J Phys Chem 1996;100:19357.
[33] Cossee P. J Catal 1964;3:80.
[34] Arlman EG, Cossee P. J Catal 1964;3:99.
[35] Lee C, Yang W, Parr RG. Phys Rev B 1988;37:785.
[36] Niecke E, Becker P, Nieger M, Stalke D, Schoeller WW. Angew Chem Int Ed Engl 1995;34:1849.
[37] Rappé AK, Casewitt CJ, Colwell KS, Goddard WA, Skiff WM. J Am Chem Soc 1992;114:10024.
[38] Frisch MJ, Trucks GW, Schlegel HB, Scuseria GE, Robb MA, Cheeseman JR, et al. Gaussian 03, revision D.01. Wallingford, CT: Gaussian, Inc.; 2004.
[39] Crystal data for **L5**: $C_{23}H_{23}N_3O_2$, $M = 373.44$, Orthorhombic, space group Pbca, $a = 16.322(6)$ Å, $b = 15.087(6)$ Å, $c = 33.368(13)$ Å, $\alpha = 90°$, $\beta = 90°$, $\gamma = 90°$, $V = 8217(5)$ Å^3, $Z = 16$, $D_c = 1.207$ g/m^3, $F(000) = 3168$, $1.94° < \theta < 25°$, $-19 \le h \le 12$, $-17 \le k \le 17$, $-39 \le 1 \le 35$, $T = 293$ K, yellow−brown block, $0.48 \times 0.44 \times 0.41$. $R_1 = 0.0890$ ($[I > 2\sigma(I)]$), 0.1649 (all data), $\omega R_2 = 0.1965$ ($[I > 2\sigma(I)]$), 0.2581(all data). Crystallographic data for the structures in this paper have been deposited with the Cambridge Crystallographic Data Centre as supplementary publication numbers CCDC 632007. Copies of the data can be obtained, free of charge, on application to CCDC, 12 Union Road, Cambridge CB2 1EZ, UK [fax: +44 1223 336033 or e-mail: deposit@ccdc.cam.ac.uk].
[40] Zhao T. Protonic nuclear magnetic resonance spectroscopy. Beijing: Peking University Press; 1983. p. 35.
[41] Muetterties EL, Phillips WD. The use of NMR in inorganic chemistry. Adv Inorg Chem Radiochem 1962;4:231.
[42] Vreven T, Morokuma K, Farkas Ö, Schlegel HB, Frisch MJ. J Comput Chem 2003;24:760.